

# Zone-Drawing and Zone-Annealing of Poly(L-lactic acid) Microfiber Prepared by CO<sub>2</sub> Laser-Thinning Method

Akihiro Suzuki, Daisuke Mizuochi

*Interdisciplinary Graduate of School of Medicine and Engineering, University of Yamanashi, Kofu 400-8511, Japan*

Received 26 September 2005; accepted 7 January 2006

DOI 10.1002/app.24201

Published online in Wiley InterScience (www.interscience.wiley.com).

**ABSTRACT:** A zone-drawing and zone-annealing method was applied to the poly(L-lactic acid) (PLLA) microfiber obtained by using a carbon dioxide (CO<sub>2</sub>) laser-thinning to develop its mechanical properties. The microfiber used for the zone-drawing and zone-annealing was prepared by winding at 800 m min<sup>-1</sup> the microfiber that was obtained by irradiating the laser at 8.0 W cm<sup>-2</sup> to an as-spun fiber supplied at a speed of 0.5 m min<sup>-1</sup> and had a diameter of 1.5 μm and a birefringence of 20.3 × 10<sup>-3</sup>. The zone-drawing was carried out at a drawing temperature of 85°C under an applied tension of 150 MPa, and the zone-annealing at an annealing temperature of 110°C under 181 MPa. The zone-drawing and the zone-annealing were carried out at a treat-

ing speed of 0.1 m min<sup>-1</sup>. The diameter of microfiber decreased, and its birefringence increased stepwise with processing. The zone-annealed microfiber finally obtained had a diameter of 1.2 μm, a birefringence of 43.3 × 10<sup>-3</sup>, a tensile modulus of 14.0 GPa, and a tensile strength of 1.5 GPa. The wide-angle X-ray diffraction pattern of the zone-annealed microfiber showed the existence of the highly oriented crystallites. © 2006 Wiley Periodicals, Inc. *J Appl Polym Sci* 102: 472–478, 2006

**Key words:** poly(L-lactic acid); microfiber; carbon dioxide laser; mechanical properties; zone-drawing and zone-annealing; WAXD

## INTRODUCTION

The microfibers are very valuable from the viewpoint of industrial and medical materials, and are now manufactured by highly skilled techniques such as a conjugate spinning, an islands-in-a-sea-type fiber spinning, a melt blowing, and a flash spinning.<sup>1–4</sup>

The new preparation method of microfiber based on an entirely different conception from the conventional methods was developed by us. The developed method was carried out by irradiating a continuous-wave carbon dioxide (CO<sub>2</sub>) laser to fibers. The fiber is locally melted by the irradiation of the high output power laser, and that the instantaneous plastic flow occurs after the melt viscosity becomes low sufficiently. The cold drawing occurring after the instantaneous plastic flow induces the molecular orientation and crystallization in spite of a large deformation just like in the flow drawing and then gives the oriented microfiber. The thinning by the laser-heating can be considered as a die-less spinning.

The CO<sub>2</sub> laser-thinning method easily yields microfibers without using highly skilled techniques, and it is suitable for producing microfibers of various poly-

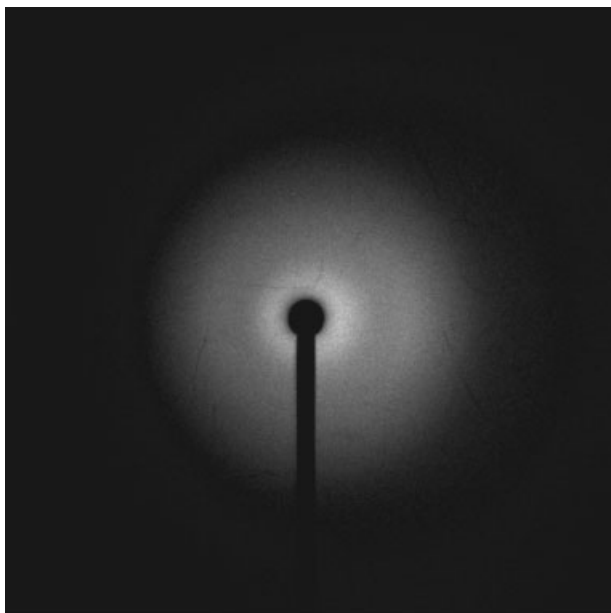
mers at a small scale. The CO<sub>2</sub> laser-thinning method was previously applied to poly(ethylene terephthalate) (PET),<sup>5,6</sup> nylon 6,<sup>7</sup> nylon 66,<sup>8</sup> isotactic polypropylene,<sup>9</sup> and poly(L-lactic acid) (PLLA),<sup>10</sup> and then their microfibers with a diameter of about 2 μm were obtained. SEM showed that the laser-thinned (LT) microfibers had smooth surfaces not roughened by laser ablation, which were uniform in diameter. The change in the molecular weight during the CO<sub>2</sub> laser-thinning hardly occurred as compared with its melt spinning.<sup>11</sup>

Although the CO<sub>2</sub> laser-thinning was characterized by the plastic flow accompanied by a molecular orientation and a strain-induced crystallization, the mechanical properties of the obtained microfiber were insufficient because of the lack of the highly oriented amorphous chains and crystallites.<sup>5–10</sup> Therefore, it was necessary to draw and anneal the microfiber obtained to improve its mechanical properties.

To improve the mechanical properties of fibers and films, a zone-drawing and zone-annealing method was developed in our laboratory. In this method, the drawing and annealing were carried out by moving the thin zone-heater of about 3 mm thickness at constant speed along the fiber applied a weight. This method was previously applied to various polymers, such as PET and nylon 6 etc, to develop their mechanical properties<sup>12–16</sup> and was suitable for improving the mechanical properties of fibers and films. The zone-drawing and zone-annealing method was also applied to the PET<sup>17</sup> and nylon 66<sup>11</sup> microfibers obtained by

Correspondence to: A. Suzuki (a-suzuki@yamanashi.ac.jp).

Contract grant sponsor: Japan Society for the Promotion of Science.



## Original fiber

Figure 1 WAXD pattern of original PLLA fiber.

CO<sub>2</sub> laser-thinning to develop their mechanical properties, and then high-modulus and high-strength microfibers were obtained.

In this study, the zone-drawing and zone-annealing method was applied to the PLLA microfiber prepared by the CO<sub>2</sub> laser-thinning to prepare high-modulus and high-strength microfiber. We present here the results pertaining to the zone-drawn (ZD) and zone-annealed (ZA) PLLA microfibers.

## EXPERIMENTAL

### Material

The original fiber used in this study was an as-spun PLLA fiber with  $M_n = 80,000$  and  $M_w = 140,000$ , supplied by Unitika (Osaka, Japan). The original fiber had a diameter of 75  $\mu\text{m}$  and birefringence of  $6.3 \times 10^{-3}$ . The glass transition temperature ( $T_g$ ) and melting point ( $T_m$ ) of the as-received fiber, as measured by a differential scanning calorimetry (DSC), were 57 and 178°C, respectively. The original fiber was amorphous and isotropic from a wide-angle X-ray diffraction (WAXD) pattern as shown in Figure 1.

### Measurements

The diameter of microfiber was measured with a scanning electron microscopy (SEM). SEM micrographs of the microfibers were taken with a JSM6060LV (Jeol

Tokyo, Japan), with an acceleration voltage of 3 or 4 kV.

Birefringence was measured with a polarizing microscope equipped with a Berek compensator (Olympus Optical Co., Japan).

WAXD images of the microfibers were taken with an imaging-plate (IP) film and an IP detector R-AXIS DS3C (Rigaku Co., Akishima Japan). The IP film was attached to a X-ray generator (Rigaku Co.) operated at 40 kV and 35 mA. The radiation was Ni-filtered Cu K $\alpha$ . The sample-to-IP film distance was 65 mm. The bundle was exposed for 30 min to the X-ray beam from a pinhole collimator with a diameter of 1.0 mm.

The degree of crystal orientation ( $\pi$ ) was estimated from the half-width ( $H$ ) of the meridian reflection peak. The  $H$  value was estimated from WAXD pattern measured by the imaging-plate through the software for analyzing data.

The  $\pi$  value is given by the following equation:

$$\pi (\%) = [(180 - H)/180] \times 100$$

The DSC measurements were carried out using a Therm Plus 2 DSC 8230C calorimeter (Rigaku Co., Akishima, Japan). The DSC scans were performed within the temperature range of 25–200°C at a heating rate of 10°C min<sup>-1</sup>. All DSC experiments were carried out under a nitrogen purge. The DSC instrument was calibrated with indium.

The degree of crystallinity ( $X_c$ ) was determined from heat of fusion ( $\Delta H_m$ ) and an enthalpy of cold crystallization ( $\Delta H_{cc}$ ) as follow:

$$X_c (\%) = [(\Delta H_m + \Delta H_{cc})/93.0] \times 100$$

where 93.0 J g<sup>-1</sup> is used as the heat of fusion of the crystalline phase of PLLA.<sup>18</sup>

A thermal shrinkage was measured with a Therm Plus TMA8310 (Rigaku Co.) at a heating rate of 5°C min<sup>-1</sup>. The measurements were performed over the temperature range from 25 to 175°C. The specimens (15 mm long) were given a very small tension (5 mN) to stretch the specimen tightly.

Tensile properties were measured at 23°C and a relative humidity of 50% with EZ Graph (Shimadzu Co., Kyoto Japan). A gauge length of 20 mm and elongation rate of 10 mm min<sup>-1</sup> were used. The experimental results are the average of 10 measurements.

### Zone-drawing and zone-annealing of the microfiber bundle

It is difficult to draw and anneal only a microfiber obtained, since its diameter and its tensile strength are too small, but the microfibers in a bundle could be drawn and annealed by a zone-heating. The microfi-

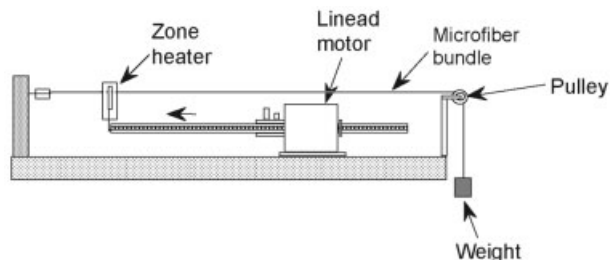


**Figure 2** Schematic diagram of apparatus used for zone-drawing and zone-annealing of microfiber bundle.

ber bundle was made by winding on a spool without a traverse in the CO<sub>2</sub> laser-thinning apparatus described previously.<sup>10</sup> To zone-draw and zone-anneal the microfiber bundle, an apparatus was specially constructed as shown in Figure 2. This apparatus consists of a temperature-controlled zone-heater and a Linead motor (Oriental Motor Co. Ltd.) capable of moving the zone heater at an arbitrary speed. One end of the microfiber bundle was connected to a fixed support while the other was connected to a weight after passing through a pulley. The drawing and annealing treatments were carried out by moving the zone-heater along the fiber direction under an optimum tension.

## RESULTS AND DISCUSSION

To improve the mechanical properties of the PLLA microfiber obtained by the laser-thinning, the zone-drawing and the zone-annealing method was applied to the microfiber with a diameter of 1.5 μm and a birefringence of  $20.3 \times 10^{-3}$ . The microfiber used in this study was prepared by winding at 800 m min<sup>-1</sup> the microfiber that was obtained by irradiating the laser at 8.0 W cm<sup>-2</sup> to the original fiber supplied at a speed of 0.5 m min<sup>-1</sup>. The microfiber obtained by the laser-thinning is designated as a LT microfiber. Preliminary experiments were carried out to decide optimum zone-drawing and zone-annealing conditions for the LT microfiber.

The purpose of the zone-drawing is to fully orient amorphous chains in the drawing direction without a thermal crystallization and to further thin the LT microfiber. The zone-drawing was carried out around the  $T_g$  to avoid any thermal crystallization because the crystallites inhibit the molecular chains from highly orienting along a drawing direction. To uniformly zone-draw the LT microfiber around  $T_g$ , the zone-drawing carried out at a treating speed of 0.1 m min<sup>-1</sup> was found to be optimum. This treating speed was used throughout the zone-drawing and the zone-annealing. The optimum condition for the zone-drawing was determined by measuring the diameter and the

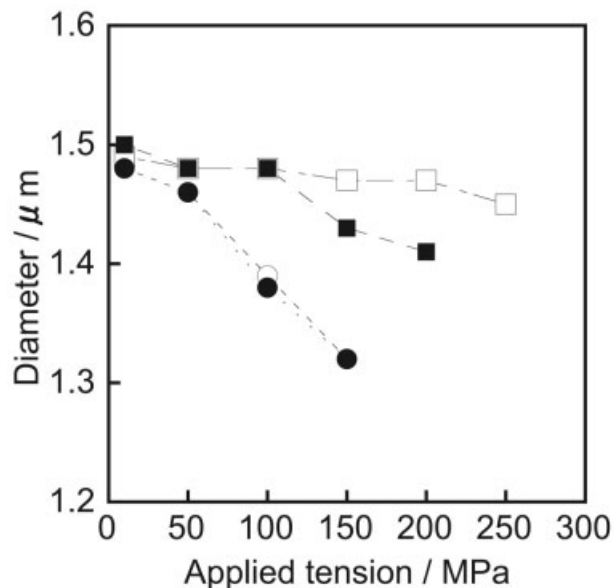
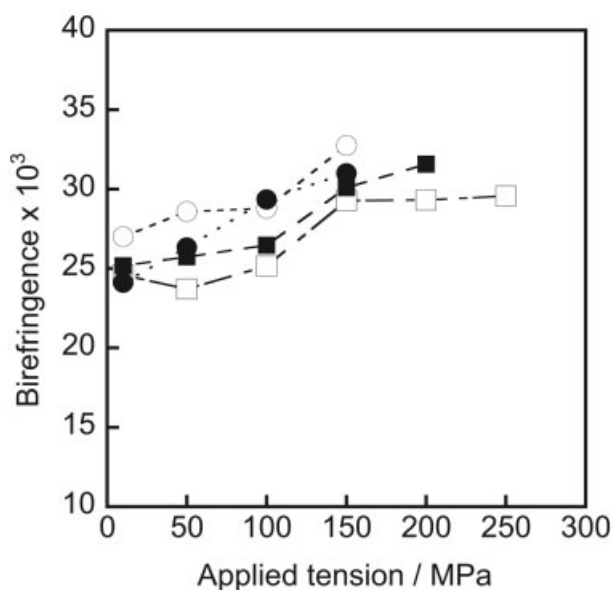


**Figure 3** Applied tension dependence of the diameters of microfibers drawn at various drawing temperatures ( $T_d$ ): □, 65°C; ■, 75°C; ○, 85°C; and ●, 95°C.

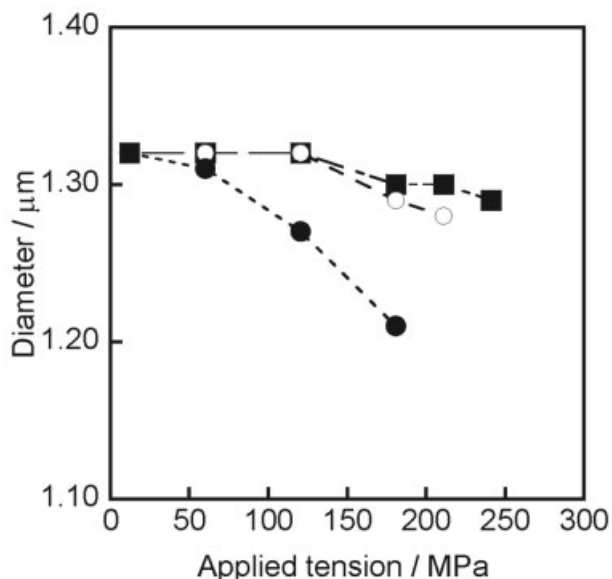
birefringence of the microfibers drawn under various conditions.

Figure 3 shows the applied tension dependence of the diameters of microfibers drawn at various drawing temperatures ( $T_d$ ) above the  $T_g$  (=57°C). The diameter decreased as the applied tension increased at each  $T_d$ , and the thinner microfiber was obtained by drawing the LT microfiber at 85 and 95°C.

Figure 4 shows the applied tension dependence of



**Figure 4** Applied tension dependence of the birefringence ( $\Delta n$ ) of microfibers drawn at various drawing temperatures ( $T_d$ ): □, 65°C; ■, 75°C; ○, 85°C; and ●, 95°C.



**Figure 5** Applied tension dependence of the diameter for the microfibers zone-annealed at three different annealing temperatures ( $T_{an}$ ): ●, 90°C; ○, 100°C; and ■, 110°C.

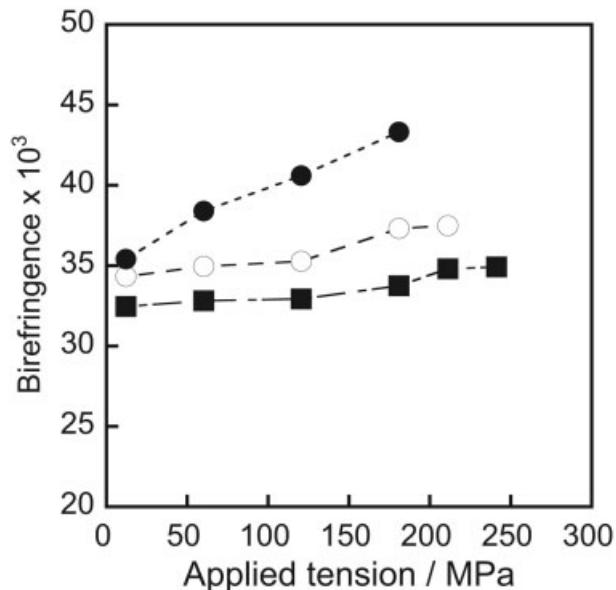


**Figure 6** Applied tension dependence of the birefringence for the microfibers zone-annealed at three different annealing temperatures ( $T_{an}$ ): ●, 90°C; ○, 100°C; and ■, 110°C.

the birefringence ( $\Delta n$ ) of microfibers drawn at various  $T_d$ 's. The  $\Delta n$  value increased with increase in the applied tension. The highest  $\Delta n$  value was  $32.8 \times 10^{-3}$  in the microfiber drawn at 85°C under 150 MPa and is equal to the intrinsic crystallite birefringence ( $\Delta n_{int} = 30 \times 10^{-3}$ ) of the PLLA.<sup>19</sup> Consequently, the condition giving the highest  $\Delta n$  value was chosen as the optimum condition for the zone-drawing. The microfiber obtained under the optimum zone-drawing condition is designated as a ZD microfiber.

The purpose of the zone-annealing is to crystallize the ZD microfiber drawn at 85°C under 150 MPa. Figures 5 and 6 show the applied tension dependence of the diameter and  $\Delta n$  for the microfibers zone-annealed at 90, 100, and 110°C. The diameter decreased with increase in the applied tension at each annealing temperature ( $T_{an}$ ), and the  $\Delta n$  value increased as the applied tension increased. The microfiber annealed at 110°C under 181 MPa had the thinnest diameter of 1.2  $\mu\text{m}$  and the maximum  $\Delta n$  value of  $43.3 \times 10^{-3}$ , and then this condition was found to be optimum to produce the thinnest microfiber. The microfiber zone-annealed under the optimum condition is designated as a ZA microfiber.

The optimum conditions for the zone-drawing and the zone-annealing are summarized in Table I. The microstructure and mechanical properties of the PLLA microfiber obtained under each optimum condition will be discussed later.

Figure 7 shows SEM photographs of the LT, ZD, and ZA microfibers. The SEM photographs at 10,000 $\times$  showed that these microfibers had smooth surfaces not roughened by laser ablation and that were uniform in diameter.

The PLLA crystallizes in two polymorphic forms:  $\alpha$  form (orthorhombic) and  $\beta$  form (trigonal).<sup>20–22</sup> The  $\alpha$  form has 10/7 helix and can be obtained by crystallization from the melt or from the solution. The  $\alpha$ - $\beta$  crystal transition took place by hot drawing and solid-state extrusion.<sup>21–23</sup>

Figure 8 shows the WAXD patterns of the LT, ZD, and ZA microfibers. The equatorial reflection due to oriented crystallites is observed in the WAXD patterns. The WAXD patterns of the ZD and ZA microfibers show strong equatorial reflections due to the highly oriented crystallites, and the strong equatorial reflections is attributable to the (0010) $\alpha$  reflection of  $\alpha$  form crystal. The WAXD pattern of the ZA microfiber shows the {(0010) $\alpha$  + (023) $\beta$ } doublet and the (003) $\beta$  slight reflection of  $\beta$  form crystal on the lower  $2\theta$  side of the doublet reflection. The sharpening of the diffraction spots indicates improvements in crystalline orientation and crystal perfection. The WAXD photograph of the ZA microfiber shows that the zone-drawing and zone-annealing achieved the high levels of crystallinity and crystalline orientation, as shown later.

**TABLE I**  
Optimum Conditions for the Zone-Drawing and Zone-Annealing

Treatment	Treating temperature (°C)	Applied tension (MPa)
Zone-drawing	85	150
Zone-annealing	110	181

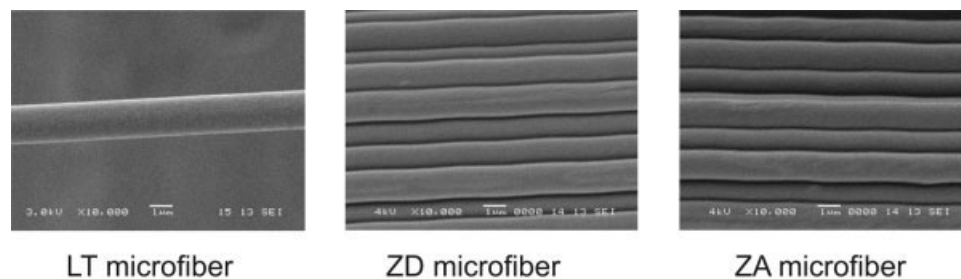


Figure 7 SEM photographs of the LT, ZD, and ZA microfibers.

Figure 9 shows DSC curves for the original fiber, LT, ZD, and ZA microfibers. The original fiber shows a change in slope in the specific heat at 62°C, which corresponds to the  $T_g$ ; an exothermic transition at 90°C caused by a cold crystallization; and a broad melting endotherm peaking at 166°C. Its melting peak can be ascribed to the lamellar crystals of  $\alpha$  form, which crystallized during the DSC scanning<sup>24,25</sup> because the  $\alpha$  form was obtained by crystallization from the melt. No melting peak of the  $\beta$  form, which is about 10°C lower than that of the  $\alpha$  crystal,<sup>26</sup> is observed in the DSC curve of the original fiber.

The LT microfiber has a cold crystallization temperature ( $T_{cc}$ ) of 72°C, a melting endotherm peaking at 169°C, and the trace of shoulder on the lower temperature side of their peaks, but the melting peak due to the  $\beta$  form was not observed in the DSC curves of the LT microfiber. The  $T_{cc}$  of the LT microfiber is 19°C lower than that of the original fiber. The decrease in the  $T_{cc}$  was caused by the increase in the degree of orientation of amorphous chains. The  $T_m$  of the LT microfiber is 3°C higher than that of the original fiber. The appearance of the shoulder on the lower temperature side of the melting peak is based on the fringed-micelle  $\alpha$  crystals formed by the flow-induced crystallization. Elenga et al.<sup>26</sup> suggested from the standpoint of kinetics that the low-temperature melting peak was ascribed to the fringed-micelle crystals built up by chain unfolding, and the high-temperature one corresponds to the untransformed fraction of the lamellar

crystals that undergo reorganization during the heating scan.

The  $T_m$  of ZD microfiber is 165 and 4°C lower than that of the LT microfiber. The drop of  $T_m$  was attributable to imperfect fringed-micelle crystals formed by unfolding the lamellar crystals during the zone-drawing process. The ZA microfiber had the higher  $T_m$  (=168°C), and the increase in the  $T_m$  was caused by the increase in the degree of crystallinity and crystallized crystals with higher perfection.

Table II lists the diameter, birefringence ( $\Delta n$ ), degree of crystallinity ( $X_c$ ), and degree of crystal orientation ( $\pi$ ) for the LT, ZD, and ZA microfibers. The  $\pi$  value estimated from the half-width ( $H$ ) of the meridian (0010) $\alpha$  reflection peak.

The diameter decreases and the  $\Delta n$  value increases stepwise with the processing, and then the ZA microfiber obtained finally has a diameter of 1.2  $\mu\text{m}$  and  $\Delta n = 43.3 \times 10^{-3}$ . The observed  $\Delta n$  value exceeds the  $\Delta n_{\text{int}}$  value of PLLA reported previously, and this was often found in other polymers such as PET.<sup>16</sup> It will be necessary to reexamine the  $\Delta n_{\text{int}}$  value of PLLA.

The  $X_c$  value increases stepwise with processing, but the  $\pi$  value was high even at the LT microfiber. The  $X_c$  value of the LT microfiber was 42% and its  $\pi$  value was 93%, although the LT fiber was obtained by an instantaneous plastic flow from the nearly molten state. The existence of the highly oriented crystallites in the LT microfiber suggested that the cold drawing

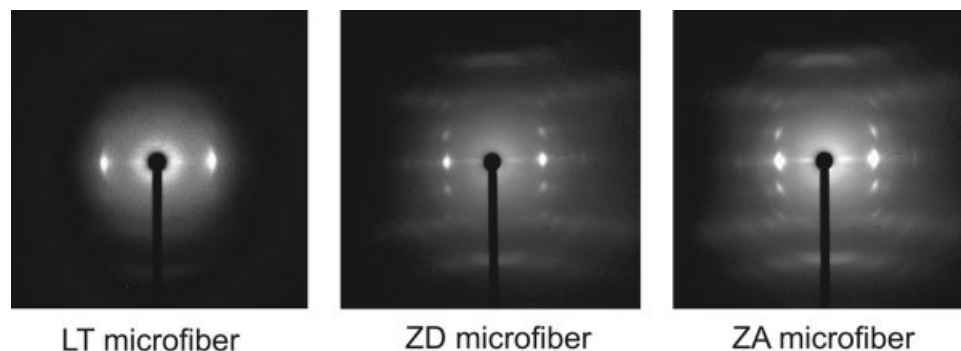
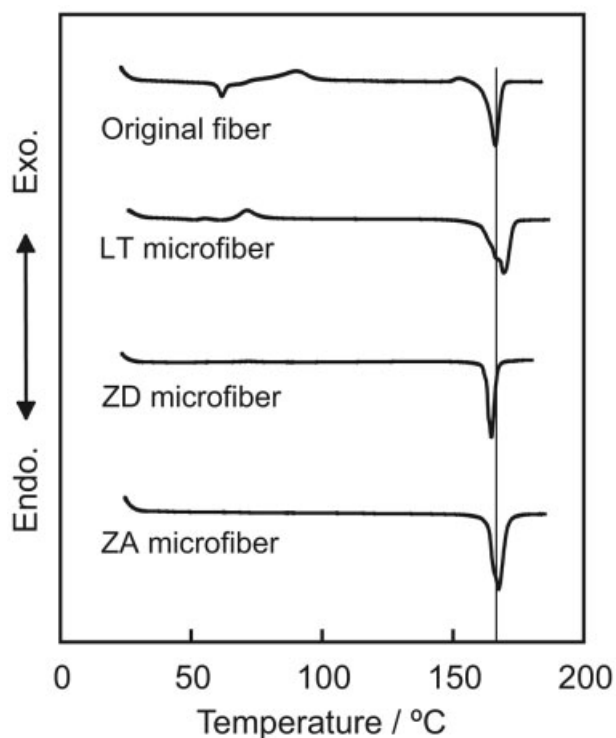


Figure 8 WAXD patterns of the LT, ZD, and ZA microfibers.



**Figure 9** DSC curves for the original fiber, LT, ZD, and ZA microfibers.

occurring after the laser heating induces the molecular orientation and the strain-induced crystallization.

The increase of  $X_c$  by the zone-drawing was mainly attributable to the strain-induced crystallization and that by the zone-annealing to thermal crystallization. The ZA microfiber finally obtained has  $X_c = 58\%$ . The  $\pi$  value already reached a high value in the LT microfiber and increased further by the zone-drawing and zone-annealing.

Figure 10 shows the temperature dependence of the thermal shrinkage for the original fiber, LT, ZD, and ZA microfibers. The development of the thermal shrinkage during heating is associated with the chain coiling in the oriented amorphous regions and is dependent on draw ratio and the degree of crystallinity. The original fiber stretches rapidly above 67°C, and the stretch exceeds the instrumental limitation after a

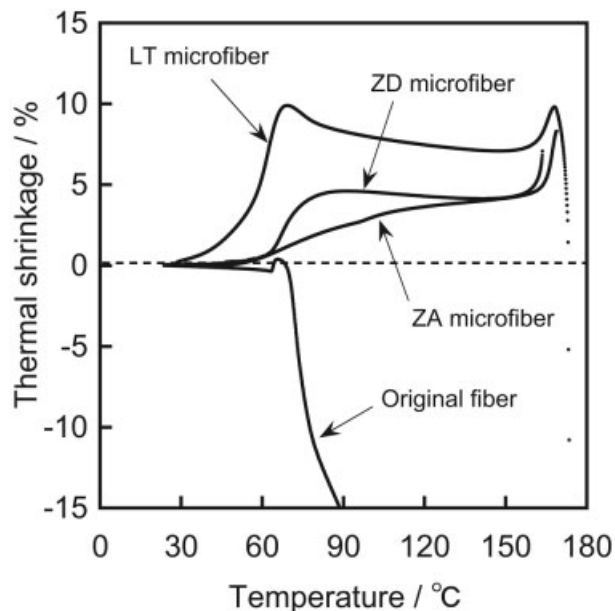


**Figure 10** Temperature dependence of the thermal shrinkage for the original fiber, LT, ZD, and ZA microfibers.

slight thermal shrinkage occurred at 64°C. The rapid stretch of the original fiber shows that no physical network, which was built up by the crystallites preventing the fluid-like deformation, exists, and that no strain-induced crystallization occurs during the measurement. The LT microfiber shrinks rapidly in the temperature range of 50–70°C, stretches gradually in the temperature range of 70–160°C, shrinks rapidly near the  $T_m$ , and then shrinks rapidly. The peak of thermal shrinkage near the  $T_m$  shows that the physical network was broken and that the fluid-like deformation occurred.

The ZD microfiber stretches gradually with increase in temperature after the rapid shrinkage occurred in the temperature range of 65–75°C, and then the rapid shrinkage takes place near the  $T_m$ .

The ZA microfiber shrinks gradually as the temperature increased and shrinks rapidly within a narrow range of temperature around the  $T_m$ . The difference in the behavior of the shrinkage between ZD and ZA microfibers mainly depends on the molecular mobility of the amorphous regions. The crosslink density of the physical network built up by the crystallites is influencing the molecular mobility in the amorphous region.

Table III lists the mechanical properties of the LT, ZD, and ZA microfibers. The tensile modulus and the tensile strength increase stepwise with increase in processing. The tensile modulus and the tensile strength of the ZA microfiber are 14.0 and 1.5 GPa, respectively.

There are many approaches to produce the PLLA fibers with high modulus and high strength. The high-

**TABLE II**  
Diameter, Birefringence ( $\Delta n$ ), Degree of Crystallinity ( $X_c$ ), and Degree of Crystal Orientation ( $\pi$ ) for the Original Fiber, LT, ZD, and ZA Microfibers

Fiber	Diameter ( $\mu\text{m}$ )	$\Delta n \times 10^{-3}$	$X_c$ (%)	$\pi$ (%)
Original fiber	75	6.3	15	–
LT microfiber	1.5	20.3	42	93
ZD microfiber	1.3	32.8	56	94
ZA microfiber	1.2	43.3	58	96

**TABLE III**  
**Mechanical Properties for the Original Fiber,**  
**LT, ZD, and ZA Microfibers**

Fiber	Tensile modulus (GPa)	Tensile strength (GPa)	Elongation at break (%)
Original fiber	2.7	0.09	–
LT microfiber	5.2	0.66	39
ZD microfiber	13.4	0.93	21
ZA microfiber	14.0	1.50	14

strength PLLA fiber with a tensile modulus of 16 GPa and tensile strength of 2.1 GPa was produced by dry spinning of a PLLA solution and a hot-drawing.<sup>27</sup> The PLLA fiber, having a tensile modulus of 9 GPa and tensile strength of 0.87 GPa, was prepared by the melt spinning and drawing method.<sup>28</sup> Melt spinning and spin drawing method prepared the PLLA fiber having a Young's modulus of 6 GPa and tensile strength of 0.46 GPa.<sup>29</sup>

The LT PLLA microfiber could be drawn and annealed by the zone-drawing and zone-annealing to improve its mechanical properties. Its mechanical properties are almost equivalent to those of the PLLA fibers with high-modulus and high-strength.

The improvement of mechanical properties is closely related to rigid amorphous regions restricted strongly by the physical network built up by the crystallites. The existence of the rigid amorphous regions is clarified by the temperature dependence of the thermal shrinkage as shown in Figure 10.

### CONCLUSIONS

The PLLA microfiber obtained by the laser-thinning was zone-drawn and zone-annealed to improve its mechanical properties. The diameter of microfiber decreased and mechanical properties increased with the zone-drawing and the zone-annealing. The ZA microfiber finally obtained had a diameter of 1.2  $\mu\text{m}$ , a birefringence of  $43.3 \times 10^{-3}$ , a tensile modulus of 14

GPa, and a tensile strength of 1.5 GPa. The zone-drawing and zone-annealing method was found to be effective in producing the PLLA microfiber with high-modulus and high-strength.

### References

- Bhat, G. S.; Malkan, S. R. *J Appl Polym Sci* 2002, 83, 572.
- De Clerck, K.; Rahier, H.; Mele, B. V.; Kiekens, P. *J Appl Polym Sci* 2003, 89, 3840.
- Zhao, R.; Wadsworth, L. C. *Polym Eng Sci* 2003, 42, 463.
- Rwei, S. P. *Polym Eng Sci* 2004, 44, 331.
- Suzuki, A.; Mochizuki, N. *J Appl Polym Sci* 2003, 88, 3279.
- Suzuki, A.; Mochizuki, N. *J Appl Polym Sci* 2003, 90, 1955.
- Suzuki, A.; Kamata, K. *J Appl Polym Sci* 2004, 92, 1454.
- Suzuki, A.; Hasegawa, T. *J Appl Polym Sci* 2006, 99, 802.
- Suzuki, A.; Narusue, S. *J Appl Polym Sci* 2006, 99, 27.
- Suzuki, A.; Mizuochi, D.; Hasegawa, T. *Polymer* 2005, 46, 5550.
- Suzuki, A.; Hasegawa, T. *J Appl Polym Sci* 2006, 101, 42.
- Kunugi, T.; Suzuki, A.; Hashimoto, M. *J Appl Polym Sci* 1981, 26, 1951.
- Suzuki, A.; Kuwabara, T.; Kunugi, T. *Polymer* 1998, 39, 4235.
- Suzuki, A.; Kohno, T.; Kunugi, T. *J Polym Sci Part B: Polym Phys* 1998, 36, 1731.
- Suzuki, A.; Chen, Y.; Kunugi, T. *Polymer* 1998, 39, 5335.
- Suzuki, A.; Toda, K.; Kunugi, T. *Polymer* 2000, 41, 6061.
- Suzuki, A.; Okano, T. *J Appl Polym Sci* 2004, 92, 2989.
- Kalb, B.; Pennings, A. J. *Polymer* 1980, 21, 607.
- Kobayashi, J.; Asahi, T.; Ichiki, M.; Oikawa, H.; Suzuki, T.; Watanabe, E.; Fukada, E.; Shikinami, Y. *J Appl Phys* 1995, 77, 2957.
- Eling, B.; Gogolewski, S.; Pennings, A. J. *Polymer* 1982, 23, 1587.
- Hoogsteen, W.; Postema, A. R.; Pennings, A. J. *Macromolecules* 1990, 23, 634.
- Miyata, T.; Masuko, T. *Polymer* 1997, 38, 4003.
- Takahashi, K.; Sawai, D.; Yokoyama, T.; Kanamoto, T.; Hyon, S. H. *Polymer* 2004, 45, 4969.
- Pecorini, T. J.; Hertzberg, R. W. *Polymer* 1993, 34, 5053.
- Quintanilla, L.; Rodriguez-Cabello, J. C.; Pastor, J. M. *Polymer* 1994, 35, 2321.
- Sawai, D.; Takahashi, K.; Imamura, T.; Nakamura, K.; Kanamoto, T.; Hyon, S. H. *J Polym Sci Part B: Polym Phys* 2002, 40, 95.
- Elenga, R.; Seguela, R.; Rietsch, F. *Polymer* 1991, 32, 1975.
- Leenslag, W. J.; Gogolewski, S.; Pennings, A. J. *J Appl Polym Sci* 1984, 29, 2829.
- Leenslag, W. J.; Pennings, A. J. *Polymer* 1987, 28, 1695.
- Schmack, G.; Tändler, B.; Vogel, R.; Beyreuther, R.; Jacobsen, S.; Fritz, H. G. *J Appl Polym Sci* 1999, 73, 2785.